# CHAPTER 10

# DISCUSSION

## 10.1 The two wear machines.

Part of the purpose of the present work was the construction of a rolling-sliding, twin disc, wear machine which would have more control than established Amsler type machines and more stable, wide ranging contact conditions for larger, standardised disc geometries. The LEROS machine was successfully constructed and available for use during the latter period of the wear test programme. Its greater range enabled stable tests to be carried out, with wide track cylindrical disc contact, under the severest test conditions encountered on rail track.

Many tests were carried out on LEROS and the modified Amsler under similar maximum contact stress ($p_o$) and creepage ($\gamma$) conditions; comparable results were produced. Although wear rates and traction coefficients were a little higher on the Amsler, material ranking was the same on both machines, together with associate microstructural features for the respective materials at each test condition. A singular difference was the formation of 0.3mm wavelength, shallow corrugations on some Amsler discs; their presence was connected to the geared drive differential of that machine.

The independent, controlled drives for each of a LEROS disc pair meant that load and speed conditions could be tuned for, and during, each test, thus giving closer control of contact stress and creepage. This facility was being devloped during the test programme. If the wear of one disc is markedly higher than that of the other, for a given machine setting, creepage can significantly deviate from the initial set value and, to a lesser extent, contact stress also deviates. Other workers quote initial contact conditions but do not mention how they have altered at the test end[eg. Devanathan and Clayton, 1991] as in the present work. Many other wear tests, comparing the performance of rail steels, have been carried out on Amsler type machines using just one initial value of creepage, i.e. that of the geared drive (eg. Ichinose et al[1978],

Masumoto et al[1978], Sugino et al[1982]). These authors quote normal load and slippage conditions only. They do not mention changes in contact stress and creepage with differential wear of the discs. The loads used have often corresponded to low values of contact stress which are not typical of (damaging) wheel-rail contact (eg. Sato et al[1993] 430 and 525 MPa $p_o$, 0%, 5.1%, 10.5% and 29.9% $\gamma$; Sugino et al[1982], 547 MPa $p_o$, 9.4% $\gamma$, Masumoto et al[1978], both 547 MPa $p_o$, 8.6% $\gamma$; Ichinose et al[1978], 548 MPa $p_o$, 9.6% $\gamma$; Akama & Matsuyama[1987], 547 MPa $p_o$, 9.4% $\gamma$). The present work has clearly shown that respective material performance can alter with creepage, and under severe conditions, quite markedly with a change in contact stress.

The wide track of LEROS discs, twice that of standard Amsler discs, gave far more uniform loading conditions across the contact between the track edges, where the compressive stress is relaxed by plastic edge collapse ("mushrooming"). This enabled the high loading facility of the machine to be used. Heavy wear of disc pairs shaped as wheel and rail[eg. Kalousek et al, 1982; Vekser et al, 1970; Jiménez et al, 1985] results in greater contact conformity and a rapid initial reduction in contact stress. Although these wear arrangements attempt to model actual wheel-rail contact, where wearing-in of the contact occurs, material characterisation with respect to set values of contact stress and creepage cannot be accurately achieved.

To test at comparably high contact stresses for wear, and also for rolling contact fatigue, workers with rolling-sliding twin disc machines, such as the Amsler, have had to reduce track widths, by machining back, chamfering or putting a radius on one disc. With disc wear and plastic deformation, control of creepage and contact stress is further reduced by such arrangements, eg. Ishida and Sato[1988], Jamison[1990], Jiménez et al[1988], and Clayton and Devanathan[1992]. To achieve maximum contact stress values in excess of 1220 MPa, during cooled Amsler tests, Clayton and Devanathan reduced disc track widths from 5mm to 3mm. Additionally, some researchers have used different widths for top and bottom discs[eg. Sato et al, 1993]; this introduces very high concentrations of contact stress at the edges of the thinner disc, as discussed in Chapter 3 and shown in Figure 3.21. Heavy wear of a radiussed disc on a cylindrical disc will also eventually result in an approach to this situation.

The use of a standard geometry for both discs on LEROS, compared with varying bottom (driving) disc diameters with creepage on Amsler type machines, may have given a small advantage to test accuracy, since Krause and Lehna[1987] found small variations in results with changes in respective disc geometries.

To conclude, subsequent to the present work, the LEROS machine has been, and is being, successfully used for further wear and rolling contact fatigue research. Research work on LEROS has formed the basis of some published work and work submitted for publication[Garnham and Beynon, 1990 {appended}; Garnham and Beynon, 1992 {appended}; Perez, 1992; Perez and Beynon, 1993; Beynon, Garnham and Sawley, 1994; Tyfour and Beynon, 1994a and b; Tyfour, Beynon and Kapoor, 1995a & b].

### 10.2 Measurement of wear.

Wear data in the present work is based on accurate (±0.0002g) measurements of weight loss rather than changes in disc geometry. This technique was far more reliable than periodically measuring disc diameters, as clearly shown in Chapter 8 (cf. Figure 8.6), particularly if disc surface undulations developed. However, this technique does not account for the plastic deformation of disc track edges where, after initial rapid deformation, the deformation rate quickly decreases as tests progress and disc material work hardens.

A parallel can be drawn with gauge face plastic deformation of rails, with the eventual formation of a lip, as described in Chapter 5. Here again, deformation is initially quite rapid but then decelerates; the lip does not repeatedly spall off and re-form. However, loss of material from the rail head profile by this process is included in the understanding of "rail wear", in addition to far more significant material loss as wear debris. However, this deformation does have a significance with respect to these results since, although carbide free bainitic steels had inferior wear resistance (by weight loss) under most conditions, deformation of their disc edges was usually less than that seen on pearlitic discs (eg. results at 1300 MPa $p_o$, 10% $\gamma$; track width spread - Table 7.2; wear rates - Figure 8.3). This situation reflects that found on British Rail[Sawley, 1988], where installed experimental bainitic rails have shown far more resistance to profile loss by deformation, as would be

expected from their mechanical properties. Therefore the inferior wear resistance of low carbon bainites, shown by these results, is slightly alleviated on track due to less profile loss from deformation. This would be of greater significance with heavy haul rail networks where rail "crushing" can be a problem (cf. Chapter 5). It should also be noted from the track width spread results, shown in Tables 6.3 and 7.2, that deformation of pearlitic (wheel tyre) driving discs was increased where they ran against the bainitic discs, sometimes to a marked degree.

### 10.3 "Facet" and corrugation formation.

*Features.*

In the present work, wear disc *corrugations* refers to the highly visual, 0.3mm wavelength undulations of a few microns amplitude, which formed on Amsler discs only (Figure 8.9a). These formed at the same wavelength at both Amsler operating speeds, thus suggesting a fine degree of "stick-slip" in the contact.

Far larger wavelength and amplitude undulations formed on both Amsler and LEROS discs. These were termed *"facets"* due to their profile and appearance (cf. the appearance of a £0.50p coin). Facets had far longer wavelengths than the Amsler corrugations, with typically between ten and forty facets forming around all, or part of, a disc circumference with amplitudes ranging from a few microns to over 0.1mm (cf. Tables 6.3 and 7.2). These formed and grew during testing, with a corresponding increase in noise and vibration, on one or both of the discs. During a few tests, after early growth, they subsequently faded away.

In two comparative Amsler tests (tests 24 and 24A; Table 6.3), halving the machine speed also halved facet wavelength, i.e., facet frequency remained constant. This suggested a connection with the vibration characteristics of the Amsler and a vibration study was started. On LEROS, facet wavelengths remained relatively constant for both machine speeds (Tables 7.2 and 7.3) and ripples formed during severe tests at similar wavelengths. A comparative vibration analysis was also carried out on LEROS.

*Undulation formation and test condition.*

In Tables 6.4 and 7.3, corrugation, facet and ripple formation (where they have formed around the complete circumference) has been mapped against test condition and test material. The maps are not comprehensive but they indicate that such undulations, with a characteristic wavelength, will form on all of the steels within a limited range of contact stresses and creepages for each steel.

With respective milder or severer conditions outside these ranges, regular facets and corrugations do not form. However, well within the severe wear regimes, large scale wear surface plastic deformation can take the form of ripples or waves (Figure 8.58). With the LEROS discs, it was noted that these too had adopted a characteristic degree of regularity, with a similar wavelength to facets. Clear parallels can be drawn with corrugation formation on rails, as discussed in Chapter 5, where material properties at and near the wear surface, wear resistance and vibrational characteristics of the track and passing wheelsets all contribute to their formation.

The peak and valley microstructures of track corrugations and coarse LEROS disc facets are markedly similar (cf. Figures 5.10, 9.14 and 9.15), with the exception being that no white etching constituent (WEC) formed on test discs. Also markedly similar were the peak and valley hardness profiles (cf. Figure 5.11 for track and Figure 9.16 for a LEROS pearlitic rail disc). Peak-valley hardness differences were not so marked on the bainite discs (cf. Figure 9.19), perhaps reflecting their greater resistance to deformation at that test condition. This work did indicate that changing rail steel may not eliminate corrugation formation, if the new material's "faceting" characteristics still fall within the track contact stress and creepage envelope, however the severity of corrugations may be reduced.

The clearest disc undulations were formed under conditions of low contact stress and high creepage (500 MPa $p_o$, 10%$\gamma$), hence these were used for the vibration analyses on both machines. It is interesting to note that nearly all descriptions of other rail steel twin-disc tests, carried out under similar loading conditions, do not mention the

formation of undulations, neither are any test disc surfaces shown (eg. Sato et al[1993] 430 and 525 MPa $p_o$, 0%, 5.1%, 10.5% and 29.9% $\gamma$; Sugino et al[1982], 547 MPa $p_o$, 9.4% $\gamma$, Masumoto et al[1978], both 547 MPa $p_o$, 8.6% $\gamma$; Ichinose et al[1978], 548 MPa $p_o$, 9.6% $\gamma$). However, Akama and Matsuyama[1987] (Amsler type tests at 547 MPa $p_o$, 9.4% $\gamma$) do mention that heavy corrugations formed on the softer of pearlitic and tempered martensite 0.75wt.%C rail disc pairs.

*Effect on wear rate.*

Undulation formation, or disappearance, did affect wear rates, but not to a significant degree. For example, a change in test speed during Amsler Test 10c (Tables 6.3 and 8.1) had no effect on the wear curve but did initiate corrugation formation. The wear curves for LEROS tests 30, 36, 37 and 38 (cf. Chapter 8, Sections 8.5 and 8.6) show the effect of facet formation, or disappearance, on wear rate. Only for the B52/W64 test is there a clear change in the wear curve and even this was not highly significant with respect to the general spread of wear results. As Frederick[1986] observed with rail corrugations (cf. Chapter 5, Section 5.8), the wear rate differential between troughs and peaks (wear was slightly higher in the troughs) was minimal compared with the overall wear of the rail, although the peaks were significantly more plastically deformed. It is probable that this deformation resulted in more pearlitic cementite plate alignment parallel to the surface on the peaks and hence wear was reduced there (this wear mechanism is further discussed later).

*Undulations and machine vibrations.*

An initial vibration analysis was described in the appended paper[Garnham, Brightling & Beynon, 1988]. Further Amsler results are given in Chapter 6 and LEROS results in Chapter 7. This author found no direct correlation between undulation frequencies and vibration accelerations of the machines, including their natural resonances, those from drive gearing and those amplified during testing (with the exception of those caused by undulation formation).

Later work by Pupaza[Pupaza & Beynon, 1994] on the same modified Amsler (moved to another location with a different machine foundation), found some correlation by

measuring vibration *displacement* rather than accelerations. (Displacement signals were too low for significant analysis on the equipment used by this author, as described in Chapters 6 and 7.) Pupaza linked Amsler facet formation to the 11th harmonic of the natural machine frequencies when running. These may have been excited by the strong vibrations from the additional flexible gearing fitted. This author found that facets formed at a higher frequency during a comparison test on a conventional Amsler machine (cf. Test 11a, Tables 7.3 and 7.4), i.e. one not fitted with flexible gearing.

### 10.4 Wear rate analysis

With rolling-sliding wear, wear rate can be expressed in terms of either the rolling or sliding. As discussed in Chapter 8, Section 8.2, most authors have measured wear rate against the distance rolled by each disk, however this ignores the element of sliding. In this work, to accommodate sliding, the *mean* distance rolled, R, was considered (equation 8.3) and distance slid, S (equation 8.4; positive for the driving disc, negative for the driven disc) which were thus connected by creepage (equation 8.5, $\gamma = S/R$). Wear data, expressed as weight loss ($\mu g$) per unit contact area ($mm^2$) per mean distance rolled (m), $Y_r$, or slid (m), $Y_s$ (equations 8.6 and 8.7), were thus similarly related by creepage,

$$Y_r = \gamma Y_s \qquad (10.1)$$

Units were rationalised to $g/m^3$. The linkage between these two expressions of wear rate and test conditions, as described by the product of $p_o$ and $\gamma$ (where $p_o$ is maximum contact stress {equation 8.1} and $\gamma$ is creepage*) was examined. (* creepage, as defined by Bolton and Clayton[1984], as the difference between the disc circumferential speeds divided by the average of the two speeds.)

Bolton et al[Bolton, Clayton and McEwen, 1982; Bolton and Clayton, 1984] linked rolling wear rates# to test conditions by two parameters; directly to the product of test variables, $p_o\gamma$, and indirectly to $T\gamma/A$, where T is tangential force and A is the contact area. (# Their wear rates were determined as weight loss per unit disc distance "rolled" for similar

air cooled tests; i.e. an expression which includes a negative sliding element for the driven {"braking"} rail disc and a positive sliding element for the driving wheel disc.) $T\gamma/A$ was seen as an expression of work done per unit contact area per unit distance rolled. With an assumption of hertzian contact, these two parameters can be linked. Equation 3.22 gives $p_o = 4p_m/\pi$, where $p_m$ is the mean contact stress. $p_m = P/A$, where P is the normal load P and A is the contact area. Multiplying by creepage, $\gamma$, gives $p_o\gamma = 4P\gamma/\pi A$. As $P = T/\mu$, where $\mu$ is the coefficient of (kinetic) friction, this can be written, $p_o\gamma = 4T\gamma/\pi\mu A$, therefore,

$$T\gamma/A = 0.25(\pi\mu.p_o\gamma) \qquad (10.2)$$

Differences in the performance of these two terms can therefore be expected, with the highly plastic nature of metal deformation in the tests and by the fact that there was not pure sliding, but a degree of tractive rolling.

Top (driven) rail disc rolling wear rates, $Y_r$, from both wear machines, are plotted logarithmically against $p_o\gamma$ and $T\gamma/A$ in Figures 10.1 and 10.2, respectively. In these plots, mild wear data form a separate group at rolling wear rates below 10 g/m$^3$; Bolton et al[1982, 1984] found a similar low wear rate grouping for some of their mild, type I, wear results. Apart from this mild wear group, whilst a general trend is clear, the data are quite scatttered, more so with $p_o\gamma$ results at higher wear rates and $T\gamma/A$ results at lower wear rates. Plotting top (driven) discs sliding wear rates, $Y_s$, logarithmically against $p_o\gamma$ (Figure 10.3) and $T\gamma/A$ (Figure 10.4) shows a slightly clearer pattern of wear behaviour. The variability of results between $T\gamma/A = 5$ and 25 MPa reflects the different combinations of $p_o$ and $\gamma$, for given value of $p_o\gamma$, within this region. This is more pronounced if the wear rates for of the bottom (driving) discs are examined, for example, $Y_s$ against $T\gamma/A$ (Figure 10.5). Here, for tests at 1800 MPa $p_o$, 1.5% $\gamma$ ($T\gamma/A$, 7.0 - 8.3MPa; log $Y_s$ around $10^4$ g/m$^3$), there was a pronounced change between top and bottom disc wear rates for all the top rail disc combinations. There were also distinct changes in microstructural behaviour; this will be discussed later. Importantly, this example illustrates the limitations of such collective plots, as the "scatter" conceals significantly different wear

behaviours, as seen in Chapters 8 and 9. Both $p_o\gamma$ and $T\gamma/A$ are not good "homogenising" factors and cannot well represent a range of testing conditions.

However, excluding the mild wear results, tentative rankings of the materials can be made by plotting these sliding wear rate results on a linear scale, as determined by least squares analysis, against values of $T\gamma/A$ between 5 and 50 MPa. These could be viewed as representing the more severe contact conditions seen on British Rail curved track.

Top disc results are shown in Figure 10.6. Beyond 50 MPa $T\gamma/A$, the low wear rate behaviour of R52 and B52 suddenly changes to higher wear rate regime. The ranking for the majority of results shows that the carbide free bainites, B04 and B20, have inferior wear resistance. Of the two low wear rate steels, although B52 shows the highest wear resistance, if wear of the counterface wheel disc is also considered in a similar manner (Figure 10.7), it can be clearly seen that all the bainitic steels, including B52, have a *detrimental* affect on wheel disc wear.

To summarise, slightly clearer wear behavioural patterns emerged by using the sliding wear expression, $Y_s$, for expressing wear rate compared with the rolling wear expression, $Y_r$. It was initially thought that these sliding wear results could be compared with those from 100% sliding, pin on disc tests, however such tests can only run with contact stress values an order of magnitude less. Perez and Beynon[1993] examined the wear behaviour of a rail steel similar to R52, plus other pearlitic rail steels, using both pin on disc pure sliding tests and LEROS rolling-sliding tests, with the latter set to operate in the mild, Type I, wear regime. The rolling-sliding ($Y_s$) results showed a closer correlation to bulk hardness (i.e. inter-lamellar spacing) than the pure sliding pin-disc results, though the general trends were similar (Figure 10.8).

**10.5 The contact condition and wear mechanism.**

In Chapter 3, the (3 dimensional) contact mechanics of the elliptical wheel on rail contact were reviewed, together with the effect of traction force due to creepage and

resultant yield within the contact. Cylindrical (2 dimensional) contact, as used for the wear tests in the present work, was comparatively described. It was felt that material characterisation, with respect to its wear performance as a rail steel, could be more simply assessed by cylindrical contact evaluation, with singular creepage in the longitudinal direction.

It was shown that, at the traction coefficients generated by these dry wear tests (between 0.32 and 0.83; Table 8.1), maximum shear stress by any criteria would be at the surface (Figures 3.13a & b and 3.24c). The shakedown maps for cylindrical rolling-sliding contact (Figures 3.27 and 3.31b) show that, for the above values of friction, material will shakedown for $p_o/k$ values around 3, dropping down to around 1.5 for high traction coefficients, where k is the yield stress in shear (half that of yield in tension). Yield stresses could not be determined for all the test materials, but the 0.2% proof stress values can be used as a guide (Table 2.3, taking $k = \{0.2\%PS\}/2$). For $p_o/k$ values of 3 to 1.5, i.e. for traction coefficients shown above, respective $p_o$ values at the shakedown limit, based on bulk mechanical properties, would be (MPa) 551 to 276 for W64, 665 to 333 for R52, 957 to 479 for B04, 1125 to 563 for B20 and 1280 to 640 for B52. Even with allowance for strain induced directional work hardening this shows that, under most of the test conditions, shakedown would have been exceeded during running-in.

Incremental strain beyond shakedown is termed "ratchetting". Bower and Johnson[1990] have shown that pearlitic steels have a distinct ratchetting behaviour, with progressively smaller increments of strain and the material eventually settling down into a closed cycle of strain (Figure 3.30). Eventual ductility exhaustion of the material will occur resulting in tensile failure. Under such conditions it can be shown that cracks will initiate at the surface, rather than just below[Cheng et al, 1994]. Ratchetting of unsupported material above an angled crack will be accelerated to form flakes. Consequent wear debris will consist of small platelets, i.e. the flake tips. These will fracture off due to tensile failure, aided by adhesive and abrasive wear forces. It has been proposed that such ratchetting mechanisms are the main cause of wear for this type of contact, rather than low cycle fatigue[Kapoor, 1994; Johnson, 1995]. Kapoor suggests

that ratchetting and low cycle fatigue are independent and competetive mechanisms. In the present work it was observed that, except for one test condition, all flake wear debris appeared to be produced by this ratchetting mechanism.

The exception was discs tested at high contact stresses where the driving W64 discs appeared to generate plate debris by a low cycle fatigue mechanism. This is further discussed later. This phenomenon similarly occurred during rolling contact fatigue tests on LEROS[Beynon, Garnham & Sawley, 1994].

**10.6 Microstructural aspects.**

*Pearlitic R52 rail.*

With traction induced shear of pearlitic microstructures, lamellar cementite becomes aligned in the strain direction by both plastic deformation and fracture, as shown in the previous chapter. The degree of fracture or plastic deformation is determined by interlamellar spacing and by attitude to the strain direction; the finer the carbide, the easier is the plastic deformation[Langford, 1977]. Wear resistance has been linked to minimizing the ferrite free path (inter-lamellar spacing for pearlite)[Clayton, 1980, Kalousek et al, 1985], thus indicating that aligned, fine lamellar structures should have high wear resistance.

When viewed in three dimensions, the wear induced alignment of pearlitic lamellar carbide is such that the fractured carbide lamellar pieces become orientated with their flat faces laying near-parallel to the wear surface; a parallel to the composite hard and soft phase situation shown in Figure 4.18. This was confirmed by this author and by Perez[1992] by comparing hardness measurments on the wear surfaces of LEROS discs with those taken on longitudinal sections through the surface; the surface measurments were significantly harder. SEM examination of Perez's discs also indicated a higher area fraction of lamellar carbide on the wear surfaces than observed in the longitudinal microsections. Exposed interlamellar ferrite on the wear surfaces, being far softer, would be rapidly worn away, thus further increasing this high area fraction of aligned hard cementite plates. In contrast, the longitudinal sections will show the average fraction of carbide, albeit re-aligned. To summarise,

due to the nature of its structure, pearlitic steel is capable of modification with directional strain resulting in improved wear resistance, particularly under certain rolling-sliding conditions. This property has also been used for steel ropes, where the highly worked pearlitic steel fibres form ropes with exceptionally high fretting resistance[Stacey, 1987; Harris et al, 1993].

The pearlitic discs wore by adhesive and abrasive removal of the ferrite and by surface initiated cracks propagating along thin layers of ferrite which had become deformed so as to lie near-parallel to the surface. These would be highly sheared and dislocated near the surface and thus low in ductility. Flattened manganese sulphide (MnS) inclusion stringers, situated within this ferrite, further facilitated crack propagation. Wear of the resultant aligned ferrite-cementite flakes would be due ductility exhaustion (at the limit of ratchetting) of material within the flake tip area and eventual fatigue fracture of these tips.

*Ductile inclusions in the pearlitic steels.*

The MnS content was less and the inclusions were finely dispersed in the bainitic steels. In the commercial pearlitic rail and wheel steels, MnS was in the usual form of large stringers. Their orientation, i.e. the grainflow, was across the track width, at 90° to the tractive force. The strain alignment of the microstructure near the surface changed their shape from a rod toward that of a flat disc ("pancake"). This resulted in highly strained MnS/ferrite boundries which became planes of weakness which facilitated flake crack propagation. However, the majority of flake cracks were solely through ferrite; MnS was too widely dispersed. Fegredo et al[1988] examined the effect of variable inclusion contents and types on a rail steel. Wear increased with the degree of MnS pancaking; this in turn was related to their initial length/width dimensions of the MnS stringers. The MnS effect was more marked with the softer rail steels tested, i.e. those capable of more severe microstructural strain. Hard, brittle inclusions were found to have a minor role with respect to wear.

*B04 (carbide free) bainitic steel.*

This structure was free from resolvable carbide and had a low volume fraction of hard MA (martensite-austenite) phase. Therefore shearing of the surface and near-surface structure, under rolling-sliding conditions, did not appear to result in much modification of the microstructure exposed at the wear surface. This surface was still predominantly ferrite and wear rates were correspondingly high. Compared with the other steels, the performance of B04 was particularly poor under the least severe wear conditions (cf. Figures 8.1, 8.2 and 8.3). Here it seems that only B04 had partially left the mild wear regime into a more severe regime. As $p_o$ and $\gamma$ were increased, its comparative performance improved. Wear debris would have been generated by adhesion, abrasion and by rapid* fracture of flakes formed from surface initiated cracks propagating through a matrix which had run out of ductility. (* Even where a worn B04 disc surface appeared comparatively smooth, sizeable B04 flakes were found caught in the environment chamber exit filter.)

*B20 (carbide free) bainitic steel.*

This had a similar structure to B04, but with a considerably higher volume fraction of hard MA phase. Again, there was only a limited modification of the structure in the surface high shear zone; no MA particles were observed to have fractured or significantly changed shape, although some compaction between strained ferrite at the wear surface occurred. Therefore, compared with the pearlitic steels, this worn microstructure presented a less significant increase in area fraction of hard phase to the wear surface. Furthermore, the hardness* of MA phase (* averaged with allowance for the mix of structure across each particle) is estimated to be around 500 HV undeformed[Bush & Kelly, 1971], whereas cementite will be between 1000 and 1500 HV, dependent upon substitutional alloy content. It is doubtful whether MA phase would work harden above 1000 HV[Angus, 1976]. This, combined with its comparatively lower area fraction at the wear surface, resulted in only comparable, or inferior, wear resistance to pearlitic rail steel under typical British Rail contact load-creepage conditions, even though B20 has far superior mechanical properties. Additionally, these experimental bainitic steels were reasonably clean and their MnS and Ti based inclusions would have played little part in the wear process. Had their inclusion

distribution resembled that of the R52 and W64 commercial steels, their wear resistance would have been further lowered.

*B52 (conventional) bainitic steel.*

Unlike the other two bainitic steels, this steel contained significant amounts of carbide. There were two types of structure; harder regions containing laths of lower bainite within an MA, or fully martensitic, phase, with the balance (i.e. by far the higher volume fraction) consisting of conventional upper bainite. Carbide within the lower bainite-martensite regions was in the form of very fine particles aligned within the lower bainite laths. These hard regions were far larger than MA phase regions in the carbide free bainites. Under tractive strain, these brittle areas did eventually deform, or, as seen in some discs, their (comparative) rigidity generated cracks along their boundaries with the upper bainite matrix, where these boundaries broke the surface (Figure 9.11). Suprisingly these cracks did not propagate and wear resistance remained high. Although these lower bainite - martensite regions did not align themselves in the manner of pearlitic steel lamellar cemetite, in the bulk upper bainitic matrix, there was alignment to a limited degree. The fine, pseudo-lamellar, inter-lath form of upper bainitic carbide appeared partly to mirror the alignment of pearlitic lamellar carbide. The combination of these two structures within the B52 bainite resulted in high wear resistance through a combination of aligned carbides, high volume fraction of hard phase and work hardening. However, the primary wear mechanism was again flaking from shallow angled surface initiated cracks, similar to those of the other steels, i.e. the material at the surface had ratchetted to the limit of its ductility (at the flake tips).

*Where pearlitic steel wear was high.*

A detrimental aspect of B52, and to a lesser extent the other bainites, was the high wear of their counterface W64 (wheel steel) discs. It was thought that the dispersed hard phase regions on the surfaces of the bainitic steel discs partially disrupted the (protective) alignment of the W64 pearlitic structure (eg. Figure 9.12) thus moving the steel's wear performance more towards that typical of a steel with the mechanical properties of R52 and W64.

The stress distribution of the driving W64 discs differed from that of the top driven discs (Figure 8.7). The mouth of driving wheel flake cracks entering the roll gap was subject to a crack opening displacement, whereas those of the driven wheel were compressed at entry. The W64 structures were comparatively less aligned, more susceptible to roughening and more susceptible to low cycle fatigue ("block") fracture of a larger part of the flake, than seen on the driven R52 discs (eg. Figure 9.28). This stress state difference and resultant fatigue wear became marked under the test condition of 1800 MPa $p_o$ and 1.5% $\gamma$, where all counterface W64 driving discs wore very quickly (Figures 8.2 and 8.3, Tests 46 to 49), producing large plates of debris (Figures 8.39 and 8.40). The wear rate of all the counterface driven discs, both bainites and pearlite R52, was far less. A similar sudden change, with similar contact conditions, was found during rolling contact fatigue testing on LEROS of a range of pearlitic rail steels[Beynon, Garnham and Sawley, 1994]. Angled MnS inclusions in the W64 discs facilitated both wear mechanisms, namely, surface flake crack propagation and low cycle fatigue fracture.

*Further comment on microstructures.*

The comparatively high toughness and high tensile strength of B04 and B20, shown in Figure 2.21, were partially due to the absence of carbide in these structures, as in pearlitic steel and B52 bainite, carbide-ferrite interfaces are preferential locations for micro-crack formation prior to failure. In contrast, the presence, modification and alignment of carbide in these steels is fundamental to their superior wear resistance under the rolling-sliding test conditions described here.

The wear performance of non-aligned pearlitic structures can be gauged from the poor resistance to impact wear of the nose in pearlitic steel rail crossings (cf. Chapter 5). Here, low carbon, carbide free bainitic steel crossings give better impact wear resistance.

**10.7 Work by other authors.**

In pure sliding, cooled pin-on-disc tests, Clayton et al[1987] found that bainitic steels had comparable wear perfomance to pearlitic rail steels. Under the test conditions described in this thesis, the key factor in the comparatively good wear resistance of the pearlitic steels was that the shear component, generated by rolling-sliding contact, which allowed the re-alignment of pearlitic carbide lamellae to occur without too much disruption at the wear surface. Where the creepage generated shear component was missing (eg. Amsler test 12 at 0% $\gamma$, microsection, Figure 9.1) microstructural re-alignment was minimal. With pure sliding, pin on disc tests, disruption of the aligned pearlitic wear surfaces would be more likely and, as a consequence, such comparatively high wear resistance of pearlitic steel, compared to the bainitic steels, would not be expected.

In Chapter 5, Section 5.2, the categorisation of Amsler wear results by Bolton et al[1982] and Bolton and Clayton[1984], for pearlitic rail steels, is described. They produced a transition chart for mild type I wear to severe type II wear; this is shown in Figure 10.9. According to this, many of the results in the present work fall within this transition zone. If very severe pearlite-on-pearlite tests had been carried out, where carbide alignment would have been comprehensively disrupted, the wear resistance of the pearlitic steels, compared with carbide free bainites, would have been far lower and disc wear patterns would have matched Bolton et al's ("catastrophic") type III wear. Their micrograph of a longitudinal section through a type III wear Amsler disc, Figure 10.10, shows some near surface matrix alignment, however the surface is broken up and undulating. This was a 0.73 wt% C (fine pearlitic) rail steel severely tested at 1250 MPa $p_o$ and 34% $\gamma$. Of the results reported in the present work (Figures 8.4 and 8.5), only Amsler test 13 (474 MPa $p_o$, 25% $\gamma$) began to approach this high creepage condition for a pearlitic steel. This had a comparatively high wear rate. Under these conditions, Amsler test control was limited and no further, similar tests were undertaken; partially comparative, severe bainite tests were carried out with the same $p_o\gamma$ value, but at a lower $\gamma$ (Figures 8.4 and 8.5, tests 13A and 13B).

Weston[1987], at British Rail Research, compared the rolling-sliding wear properties of 0.09wt.%C (carbide free) bainites, which BR use for crossings and bainitic wheels, with standard pearlitic rail and wheel steels. The bainites were standard crossing material (342 HV hardness), a wheel material (256 HV), an enhanced crossing material (377 HV) and the latter tempered to give carbide precipitation hardening (424 HV). The Amsler tests were at 1000 MPa $p_o$ between creepages of 1% and 15%. All the bainites had higher wear rates than the pearlitic rail steel. Weston could not correlate the appearance of the bainitic wear tracks with the type I, II, and III wear regimes of Bolton et al[1982, 1984]. At the lower creepages, surfaces were relatively smooth with flake debris small in size. As creepage increased, tracks became ripples and at the highest creepages, tracks were roughened with material scooped out and large flake debris. Wear rate vs. creepage was a smooth curve for the bainites without the discontinuity observed in the pearlite curves, which has been associated with a wear regime change. Although the bainitic wear rates were higher, the surface flakes were comparatively thinner (eg. 10μm cf. 15μm for one test condition). It was concluded that bainite flakes were fractured off more easily. The worn surface hardness of bainite discs was found to be between 500 and 627 HV0.1, in contrast to values around 760 HV0.1 for the pearlite BS11 discs. Above 3% creepage all the bainitic steels work hardened up to a similar surface hardness value of around 620 HV, irrespective of their bulk hardness. The greater surface hardening of pearlite was found to be confined to within just 10μm of the surface.

Devanathan and Clayton[1991] have carried out air-cooled Amsler tests on bainitic steels at high creepage (starting at 35%, any changes with differential disc wear rates were not given) and at maximum contact stresses between 500 and 1200 MPa. Two of the bainites were supplied (by this author and British Rail) subsequent to this work and are the same material, B04 and B52. Their third bainite had a carbon content of 0.1 wt.%. Their high creepage tests showed a reversal of the material wear resistance ranking found in the present work, with the lowest carbon bainite, B04, having the highest wear resistance. The wear regime at such high creepage is thought to be different from those described in the present work. Judging by the poor wear resistance of bainitic steels installed in curved track on British Rail[Sawley, 1986], it

would seem that the lower creepages used in the present work are a better simulation of wheel-rail contact, for high-speed passenger rail networks, than the 35% plus creepage which produced superior bainitic wear resistance for Devanathan and Clayton. Their results may be more applicable to gauge face contact conditions on heavy haul rail networks. It is difficult to understand why the 0.04%C, carbide free B04 bainite (bulk hardness 29 $R_c$, 1.93% Ni, 2.76% Cr) performed better than the 0.1%C bainite (bulk hardness 35 $R_c$, 4.09% Ni, 1.71% Cr) and B52 bainite (bulk hardness, 38 $R_c$, 1.44% Ni, 1.70% Cr), unless there was an alloying effect within the MA regions under these wear conditions. Comparing B04 and a pearlitic steel, both with the same initial hardness of around 280 HV and tested at 1220 MPa $p_o$, the authors found the B04 wear surface to have a Knoop hardness of 507 HK, compared with 402 HK for the pearlitic steel. They make a connection with the high work hardening rate of B04 and the high post-yield ductility of the carbide free bainites (cf. Figure 2.21a). An additional material feature found by these authors was the presence in B52 bainite of precipitates at prior austenite grain boundaries. These were thought to be $Fe_{23}(CB)_6$ iron borocarbides of a size 0.04-1.00 μm wide and 1.6-2.8 μm long. They found that B52 cracked along these regions as well as along the boundary between its two phases, as observed in the present work.

Several other authors have examined alternatives to the pearlitic rail steel structure. Kalousek et al[1985] heat treated a 0.72% C, 0.81% Mn rail steel to give pearlitic, upper bainitic and tempered martensitic structures, all at three hardness levels, 372, 412 and 446 HV. The materials were rolling-sliding tested on the scaled rail-wheel contact twin disc machine shown in Figure 5.14. A maximum contact stress of 1800 MPa was used. Tests were run for long periods, with changes to yaw angles and some disc reversals (to simulate single line, heavy haul track conditions). Equivalent longitudinal, lateral and spin creepage values were not given. Dry wear rates decreased significantly with hardness for martensite and bainite. Pearlite was nearly independent of hardness and had superior wear resistance to the other two structures. Electron microscopy showed that at, and near, the wear surface, fine sub-structures develop with cell sizes less than one micron in diameter. Pearlite had a particularly fine sub-structure. These authors and Heller and Schweitzer[1982], have all found

similar sub-structures in worn rails.

This work of Kalousek et al was further explored by Clayton and Devanathan[1992]. A similar premium rail steel was isothermally heat-treated to produce four microstructures (pearlite, upper bainite, upper and lower bainite, and lower bainite) for comparisons of wear resistance in the type III wear regime. The pearlite and upper bainite structures had similar values of bulk hardness around 39 HRC (≡ 380 HV[# conversion to ASTM E-140]. Upper and lower bainite, and lower bainite, microstructures had bulk hardness values of 49 HRC (# 498 HV) and 54 HRC (# 577 HV), respectively. The steels were subject to cooled Amsler tests, running against a conventional wheel steel, under severe (targeted type III) conditions. These were 35% to 50% $\gamma$ and $p_o$'s of 700, 900, 1080, 1220, 1272, 1575 and 1645 MPa. To obtain $p_o$ values $>1220$ MPa, tracks widths were reduced to 3mm. For a common hardness of around 380 HV, pearlite performed much better than upper bainite, thus confirming Kalousek's work and in line with the results in this present work. However, they found that the upper and lower bainite structure exhibited far greater resistance to wearing in the type III regime and the lower bainitic structure did not enter this wear regime, even under the severest conditions. They concluded that such bainitic structures (note, not carbide free) should be further explored for severe rail applications.

Heller and Schweitzer have compared pearlitic and bainitic rails both on track[1980] and on a twin disc machine[1982]. On track, both high strength upper bainitic steels (0.3wt.% C, 412-489 HV hardness) and low carbon, acicular, carbide-free bainitic steels (0.07wt.% C, 285-364 HV hardness) were compared with a standard 0.75wt.% C pearlitic rail steel (263 HV hardness). {Note, hardness figures are taken from the laboratory test paper[1982].} On tight curves, the pearlitic rail was superior to both bainites, "even the higher strength bainite" (their words). However the bainitic rails showed far higher resistance to plastic deformation; they were thought suitable for special applications only, such as rail crossings. The same steels, plus other harder pearlitic steels with finer structures, were examined in the laboratory on both a pin-on-disc, pure sliding wear machine and on a twin disc, rolling-sliding wear

machine. Disks for the latter were both 40mm in diameter and 10mm wide and they were run at 525 MPa $p_o$ and 0.7% slippage - i.e., very mild conditions. A clear correlation with hardness was found for the pearlitic rails; they state that no clear-cut results were obtained for the bainites and the reader is referred back to the track results described above.

Ichinose et al[1978] also carried out some limited, Amsler type tests (all at 548 MPa $p_o$, 9.6% $\gamma$) on these three types of microstructure. They heat-treated a 0.68C rail steel to give three structures at one hardness level. Their wear resistance ranking was pearlite superior to tempered martensite, which in turn was superior to bainite. From TEM examination of worn structures (via carbon replicas), they too reasoned that the difference was mainly due to the alignment, distribution, shape and size of hard phases in the microstructures within 0.3mm of the wear surface. Their bainites, all around 0.3wt.%C and between 276 and 345 HV hardness, had coarse upper bainitic structures.

Akama and Matsuyama[1987], using both pure sliding tests and rolling-sliding tests on an Amsler type machine at 547 MPa $p_o$ and 9.4% creepage, compared the wear resistance of a 0.75wt.%C rail steel structure in its usual pearlitic condition, in a slack quenched, finer pearlitic condition and, at equivalent hardness to the latter, in a tempered martensitic condition. With both types of wear test, fine pearlite was clearly more wear resistant than tempered martensite. They similarly suggested that pearlite lamellae alignment and planar condensation gave these good wear properties, additionally stating that such alignment restricted flake crack growth, and hence debris thickness, to extremely shallow angles compared with the martensitic wear. The finer debris produced by the pearlite was more easily oxidised and this in turn further restricted the adhesive wear mechanism.

The uniqueness of pearlite, in resisting rolling-sliding wear forces under mild to severe conditions, was found due to the ability of this lamella form of hard phase to align, so as to resist wear. Langford[1977], in a study of cold drawn pearlitic wire, equated pearlite strength to inter-lamella spacing. He found that pearlite strain-

hardened as an exponential function of true strain, whereas with ferrite the function was linear. He also found that cementite plates would plastically deform if thinner than 0.01microns. Compaction of the highly dislocated ferrite between the cementite plates was found to limit recovery, i.e. the growth of new, "soft" grains. In addition, he looked at upper bainitic structures; in microstructures worked to high strains it was difficult to distinguish between the deformed and fractured cementite plates of upper bainite and pearlite. This suggests perhaps, similar wear resistance mechanisms to those seen in this work for R52 and the upper bainitic regions of B52.

A recent publication[de Boer et al, 1995] has described the successful use of bainitic rails for the heavy haul, iron ore railway between Kiruna and Narvik in Lapland, where steep gradients and tight curves generate very high tractive forces on the gauge face of outer rails in curves. Their 0.41wt.%C steel, with a hardness around 440 HV, had a fine grained structure of 100% lower bainite. Its service life (i.e. gauge face wear resistance) was reported as 60% better than pearlitic head-hardened rail (380 HV hardness) and 800% better than standard, premium pearlitic rail (285 HV hardness). Good weldability was an added bonus. No mention was made of wheel wear.

**10.8 Concluding comment.**

Pearlitic steels are capable of considerable microstructural modification under rolling-sliding conditions compared with carbide-free bainitic steels. The pearlitic steel microstructural modification is enhanced by the use of finer lamellar structures where lamellar spacing has an inverse linear relatioship to hardness. The linear aspect of inter-lath carbide in upper bainitic structures means that similar modification can be approached, however this structure is more resistant to strain alignment and it has been clearly shown[Clayton and Devanathan, 1992] to have inferior rolling-sliding wear resistance to pearlitic steels when of equivalent hardness and chemical composition. The present results have shown that although such a structure may have reasonable wear resistance, it may adversely affect the wear of any pearlitic counterface body. Fine pearlite appears to be the best material for resisting wear in the dry rolling-sliding wheel-rail contact conditions found on high-speed passenger

rail networks.

During the last few years, improvements in wear (and fatigue) resistance have been achieved by controlled cooling of the rail head to give thinner carbide lamellae. Additionally, this present work has shown that lowering the concentration of large MnS stringers should also further improve the wear resistance of both rail and wheel.

These results have not shown that bainitic steels have particularly poor rolling-sliding wear resistance, with respect to their mechanical properties, just that the form of the pearlite structure facilitates a directional, microstructural modification giving it a wear resistance far in excess of that expected from its mechanical performance.

Under severe conditions, where this pearlitic microstructural alignment is disrupted at the wear surface, and/or where the low cycle fatigue strength of work hardened surface is exceeded, the wear behaviour of pearlite, compared with bainitic steels, becomes more closely related to bulk mechanical properties.

Carbide-free bainitic steels may have a role on heavy haul rail track because of their high resistance to bulk plastic deformation ("crushing") of the rail head and, judging from the results of Devanathan and Clayton[1991], in resisting extremely high creepage at the gauge face. Conventional bainitic steels structures containing lower bainite have also been shown to resist severe wear conditions[Clayton and Devanathan, 1992; de Boer et al, 1995] exceeding even those normally found on heavy haul track, however this work does not mention wear of the counterface wheel. The present work has clearly shown that this can be adversely affected by hard bainitic structures. Clayton's results, together with the results of this work, require further investigation, both in the laboratory and on track. The easy weldability of bainitic steels is another reason for further exploration of their use as rail track.

**10.9 References**


Akama, M. and Matsuyama, S. (1987). "Wear characteristics of wheel and rail steels." *Journal of JSLE Int.* No. 8, 1987, pp. 75-80.

Angus, H.T. (1976). Cast Iron - Physical and Engineering Properties. Butterworths, London.

Beynon, J.H., Garnham, J.E. and Sawley, K.S. (1994). "Rolling contact fatigue of four pearlitic rail steels." To be published. Initially submitted to *WEAR*, August 1994. Re-submitted following review, June 1995.

Bolton, P.J., Clayton, P. and McEwen, I.J. (1980). "Wear of rail and tyre steels under rolling-sliding conditions." *Proc. ASME/ASLE Lubrication Conf., San Franscisco, USA, 18-21/08/80.* Pub. *ASLE Trans.* 25 (1), pp. 17-24.

Bolton, P.J. and Clayton, P. (1984). "Rolling-sliding wear damage in rail and tyre steels." *WEAR* 93, pp. 145-165.

Bower, A.F. and Johnson, K.L. (1990). "Plastic flow and shakedown of the rail surface in repeated rail-wheel contact." *Proc. 3rd. Int. Symp. on "Contact mechanics and wear in rail-wheel systems", 22-26/7/90, Univ. of Cambridge (UK).* Pub. *WEAR* 144 (1991), pp. 1-18.

Bush, M.E. and Kelly, P.M. (1971). "Strengthening mechanisms in bainitic steels." *Acta Met.* 19, pp. 1363-1371.

Cheng, W., Cheng, H.S., Mura, T. and Keer, L.M. (1994). "Micromechanics modelling of crack initiation under contact fatigue." *Trans. ASME* 116, pp. 2-8.

Clayton, P. (1980). "The relationship between wear behaviour and basic material properties for pearlitic steels." *WEAR* 60, pp. 75-93.

Clayton, P. and Allery, M.B.P. (1982). "Metallurgical aspects of surface damage problems in rails." *Canadian Metall. Quart.*, 21 (1), pp. 31-46.

Clayton, P. and Hill, D.N. (1987). "Rolling contact fatigue of a rail steel." *WEAR* 117 (3), pp. 319-334.

Clayton, P. and Devanathan, R. (1992). "Rolling-sliding wear behaviour of a chromium-molybdenum rail steel in pearlitic and bainitic conditions." *WEAR* 156, pp. 121-131.

De Boer, H., Datta, S.R., Kaiser, H-J., Lundgreen, S.O., Müsgen, B., Schmedders, H. and Wick, K. (1995). "Naturharte bainitische Schienen mit hoher Zugfestigkeit" (Naturally hard bainitic rails with high tensile strength). *Stahl und Eisen* 115 (2), pp. 93-98 (english précis, p.138).

Devanathan, R. and Clayton, P. (1991). "Rolling-sliding wear behaviour of bainitic steels." *WEAR* 151 (2), pp. 255-267.

Fegredo, D.M., Shehata, M.T., Palmer, A. and Kalousek, J. (1988). "The effect of sulphide and oxide inclusions on the wear rates of standard C-Mn and a Cr-Mo rail steels. *WEAR* 126, pp. 285-306.

Frederick, C.O. (1986). "A rail corrugation theory." *Proc. 2nd. Int. Symp. on "Contact mechanics and wear of rail-wheel systems", Kingston, Rhode Island, USA, July 1986.* Pub. Univ. of Waterloo Press, Waterloo, Ontario, 1987. Also *WEAR* 117.

Garnham, J.E., Brightling, J.R. and Beynon, J.H. (1988). "Rolling-sliding dry wear testing - a vibration analysis." *WEAR* 124, pp. 45-63 (appended - Appendix I).

Garnham, J.E. and Beynon, J.H. (1990). "The early detection of rolling-sliding contact fatigue cracks." *Proc. 3rd. Int. Symp. on "Contact mechanics and wear in rail-wheel systems", 22-26/7/90, Univ. of Cambridge (UK).* Pub. *WEAR* 144 (1991), pp. 103-116 (appended - Appendix II).

Garnham, J.E. and Beynon, J.H. (1992). "Dry rolling-sliding wear of bainitic and pearlitic steels." *WEAR* 157, pp. 81-109 (appended - Appendix III).

Harris, S.J., Waterhouse, R.B. and McColl, I.R. (1993). "Fretting damage in locked coil steel ropes." *WEAR* 170,pp. 63-70.

Heller, W. and Schweitzer, R. (1980). "High strength pearlitic steel does well in comparative tests of alloy rails." *Railway Gazette Int.*, October 1980, pp. 855-857.

Heller, W. and Schweitzer, R. (1982). "Hardness, microstructure and wear behaviour of rail steels." *Proc. 2nd. Int. Conf. on "Heavy Haul Railways", Colorado Springs, CO, 25-29/9/82*, Assc. of American Railroads and American Soc. of Mech. Engrs., pp. 282-286.

Ichinose, H., Takehara, J., Iwasaki, N. and Ueda, M. (1978). "An investigation on contact fatigue and wear resistance behaviour in rail steels." *Proc. 1st. Int. Conf. on "Heavy Haul Railways", Perth, Australia, September, 1978.* Inst. Engrs. Austr. and Austr. Inst. Mining and Metallurgy, 1978, Session 307, Paper I.3.

Ishida, M. and Sato, Y. (1988). "Development of rail-wheel high speed contact fatigue testing machine and experimental results." *Quarterly Report of the Railway Technical Inst. Japan*, 29 (2), pp. 67-71.

Jamison, W.E. (1980). "Wear of steel in combined rolling and sliding." *Proc. ASME-ASLE Lubrication Conf., San Francisco, CA, 18-21/8/80.* Pub. *ASLE Trans.* 25 (1), 1981, pp. 71-78.

Jiménez, F.J.G. and Morollón, E.C. (1985). "Rolling wear behaviour of ferrite-pearlite UIC R7 wheel steel." *Proc. 8th. Int. Wheelset Congress, Madrid, Spain, 1985.*

Jiménez, F.J.G. and Sevillano, J.G. (1988). "An analysis of experimental results of rolling-sliding behaviour of a wheel steel." *Proc. 9th. Int. Wheelset Congress, Montreal, Canada, 1988.*

Johnson, K.L. (1995). "Contact mechanics and the wear of metals". *Proc. Mechanics Colloquium, Dept. of Engineering, Univ. of Cambridge (UK), 26/01/95.* (Submitted to *WEAR* for publication.)

Kalousek, J., Rosval, G. and Ghonem, H. (1982). "Lateral creepage and its effect on wear in the rail-wheel interface." *Proc. 1st. Int. Conf. on "Contact mechanics and wear of rail-wheel systems", Vancouver, BC, July 1982.* Pub. Univ. of Waterloo Press, Waterloo, Ontario, eds. J. Kalousek et al.

Kalousek, J., Fegredo, D.M. and Laufer, E.E. (1985). The wear resistance and worn metallography of pearlite, bainite and tempered martensite rail steel microstructures of high hardness." *Proc. Int. Conf. on "Wear of Materials '85", Vancouver, BC, 14-18/4/85.* Pub. *WEAR* 105 (3), 1985, pp. 199-222.

Kapoor, A. (1994). "A re-evaluation of the life to rupture of ductile metals by cyclic plastic strain." *Fatigue Fract. Engng. Mater. Struct.* 17 (2), pp. 201-219.

Krause, H. and Lehna, H. (1987). "Investigation of tribological characteristics of rolling-sliding friction systems by means of systematic wear experiments under well defined conditions." *WEAR* 119 (2), pp. 153-174.

Langford, G. (1977). "Deformation of pearlite." *Metall. Trans. A*, 8 (6), pp. 861-875.

Masumoto, H., Sugino, K. and Hayashida, H. (1978). "Development of wear resistant and anti-shelling high strength rails in Japan." *Proc. 1st. Int. Conf. on "Heavy Haul Railways", Perth, Australia, September, 1978.* Inst. Engrs. Austr. and Austr. Inst. Mining and Metallurgy, 1978, Session 212, Paper H1.

Perez-Unzueta, A.J. (1992). "Wear resistance of pearlitic rail steels." *PhD thesis*, University of Leicester.

Perez-Unzueta, A.J. and Beynon, J.H. (1993). "Microstructure and wear resistance of pearlitic rail steels." *WEAR* 162-164, pp. 173-182.

Pupaza, D. and Beynon. J.H. (1994). "The use of vibration monitoring in detecting the initiation and prediction of corrugations in rolling-sliding contact wear." *WEAR* 177, pp. 175-183.

Sato, M., Anderson, P.M. and Rigney, D.A. (1993). "Rolling-sliding behaviour of rail steels." *WEAR* 162-164, pp. 159-172.

Sawley, K.J.[British Rail Research, Derby, UK] (1986). Personal communication with respect to the wear of experimental bainitic rails, compared to standard pearlitic rails, installed in curved track.

Sawley, K.J.[British Rail Research, Derby, UK] (1988). Personal communication with respect to the profile loss from the gauge face of experimental bainitic rails compared to standard pearlitic rails.

Stacey, A.G. (1987). "The technology of steel wire ropes." *Metals & Materials*, 3 (12), pp. 706-711.

Sugino, K., Kageyama, H. and Masumoto, H. (1982). "Development of weldable high strength steel rails." *Proc. 2nd. Int. Conf. on "Heavy Haul Railways", Colorado Springs, CO, 25-29/9/82*, Assc. of American Railroads and American Soc. of Mech. Engrs., pp. 187-198.

Tyfour, W.R., Beynon, J.H. (1994a). "The effect of rolling direction reversal on fatigue crack morphology and propagation." *Trib. Int.* 27 (4), pp. 273-282.

Tyfour, W.R., Beynon, J.H. (1994b). "The effect of rolling direction reversal on the wear rate and wear mechanism of pearlitic rail steel." *Trib. Int.* 27 (6), pp. 401-412.

Tyfour, W.R., Beynon, J.H. and Kapoor, A. (1995a). "The steady state wear behaviour of pearlitic rail steel under dry rolling-sliding contact conditions." *WEAR* 180, pp. 79-89.

Tyfour, W.R., Beynon, J.H. and Kapoor, A. (1995b). "Deterioration of rolling-contact fatigue life of pearlitic rail steel due to dry-wet rolling-sliding line contact." Amended text re-submitted for publication in *WEAR*, February 1995.

Vekser, N.A., Kazarnovskii, D.S. and Khurgin, L.S. (1970). "Method of testing wheel and rail steels for wear and contact fatigue galling." *Ukranian Scientific Research Inst. of Metals, Zavodskaya Laboratoriya* 36 (5), pp. 598-600 (Russian); *Ind. Lab.* pp. 760-761 (English); May 1970.

Weston, J. and Sawley, K.J.[British Rail Research, Derby, UK] (1987). "Rolling-sliding wear of a range of bainitic steels." British Rail Research unpublished results, personal communication.

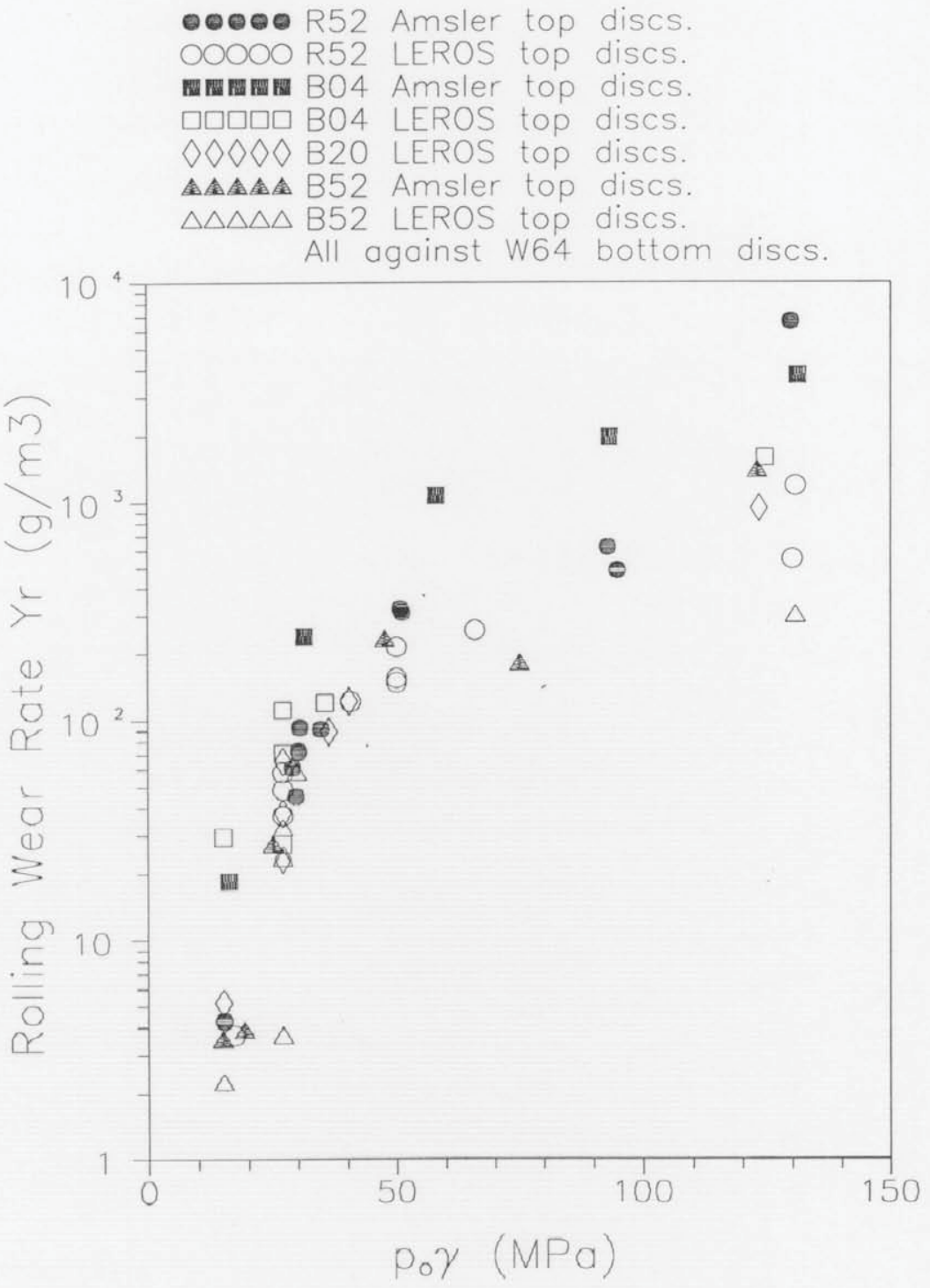


**Figure 10.1** Rolling wear rate $Y_r$ plotted logarithmically against $p_o\gamma$ for all top (driven, "braking") discs tested.

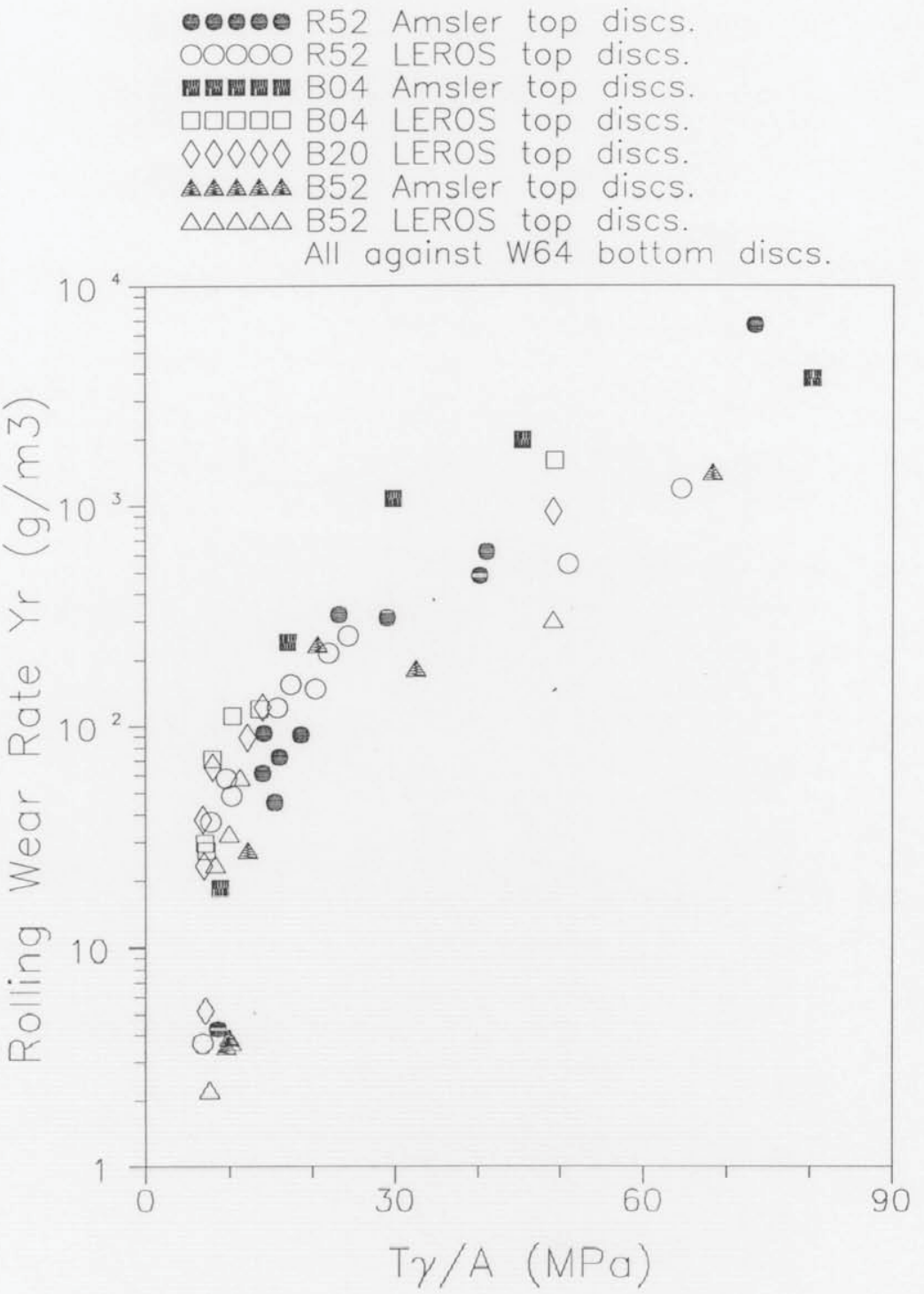


**Figure 10.2** Rolling wear rate $Y_r$ plotted logarithmically against $T\gamma/A$ for all top (driven, "braking") discs tested.

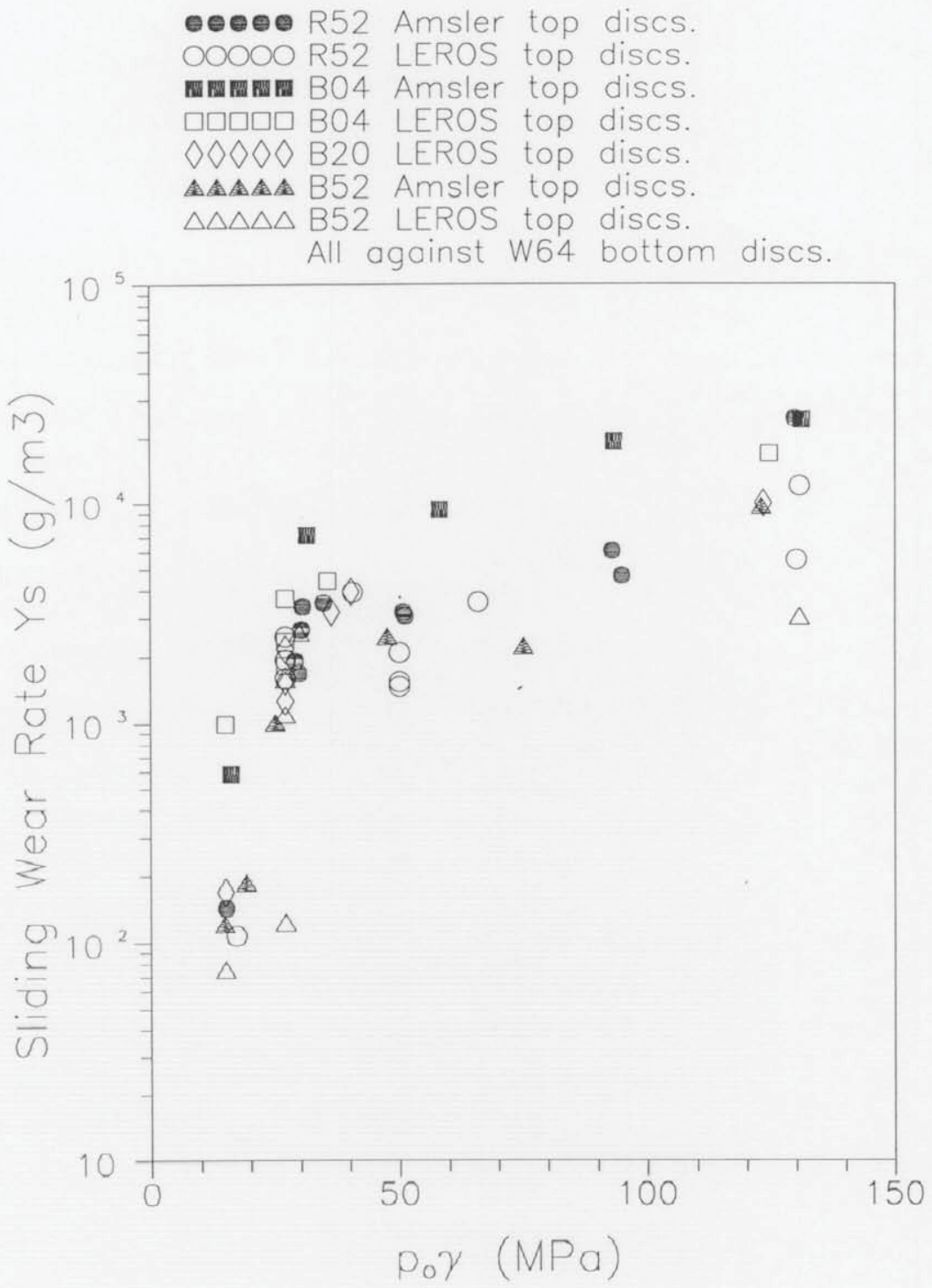


**Figure 10.3** Sliding wear rate $Y_s$ plotted logarithmically against $p_o\gamma$ for all top (driven, "braking") discs tested.

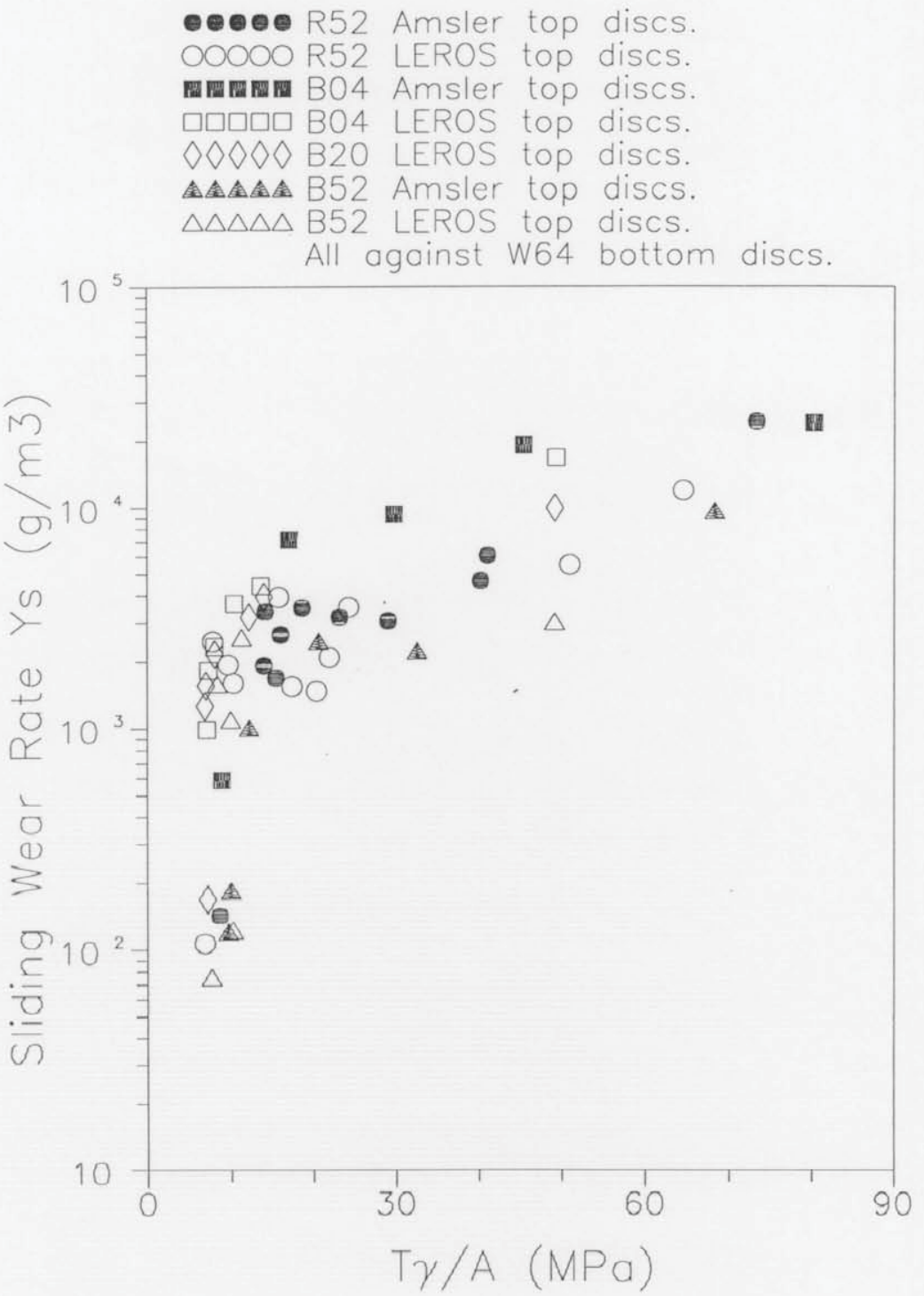


**Figure 10.4** Sliding wear rate $Y_s$ plotted logarithmically against $T\gamma/A$ for all top (driven, "braking") discs tested.

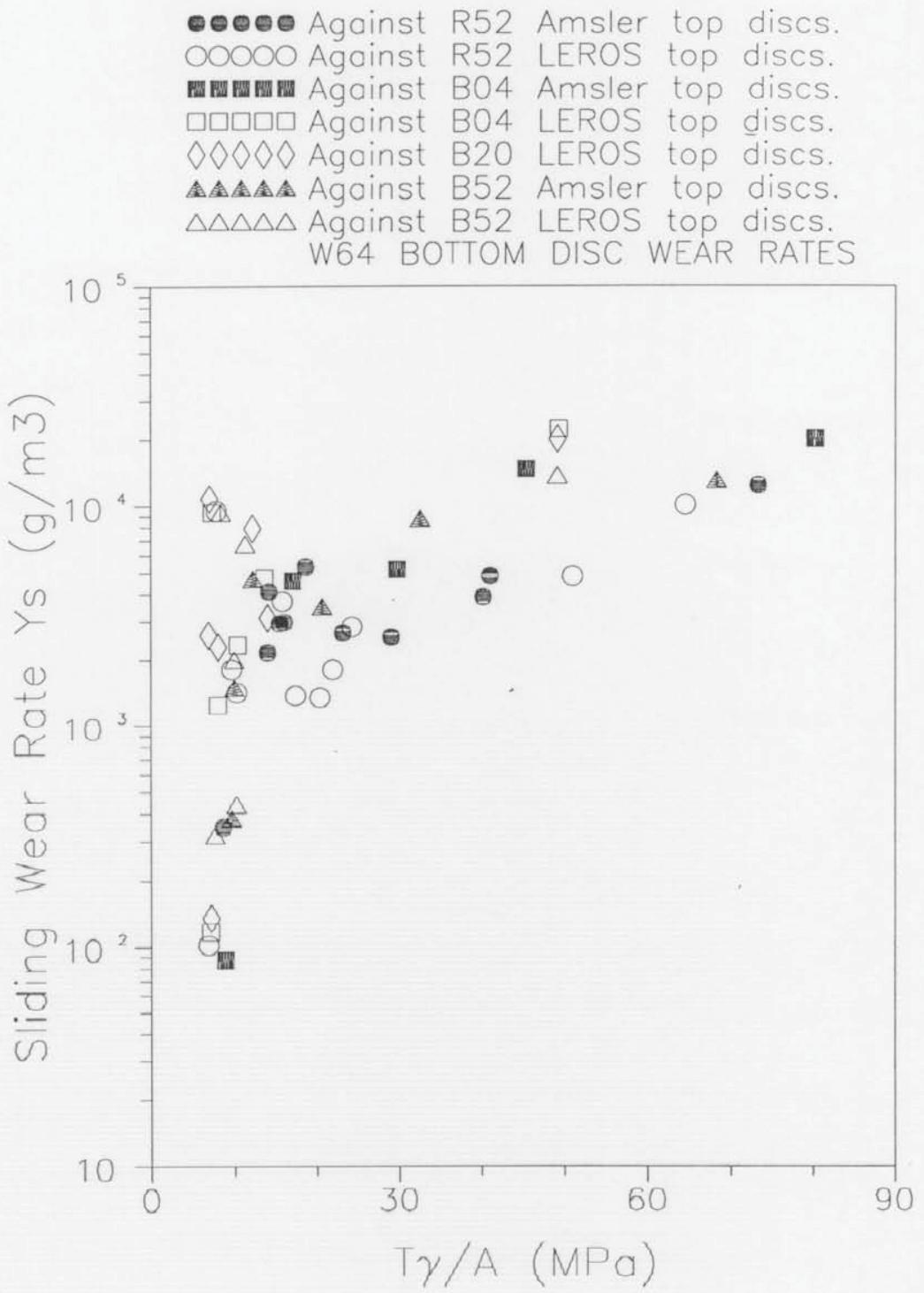


**Figure 10.5** Sliding wear rate $Y_s$ plotted logarithmically against Tγ/A for all bottom (driving) W64 discs tested.

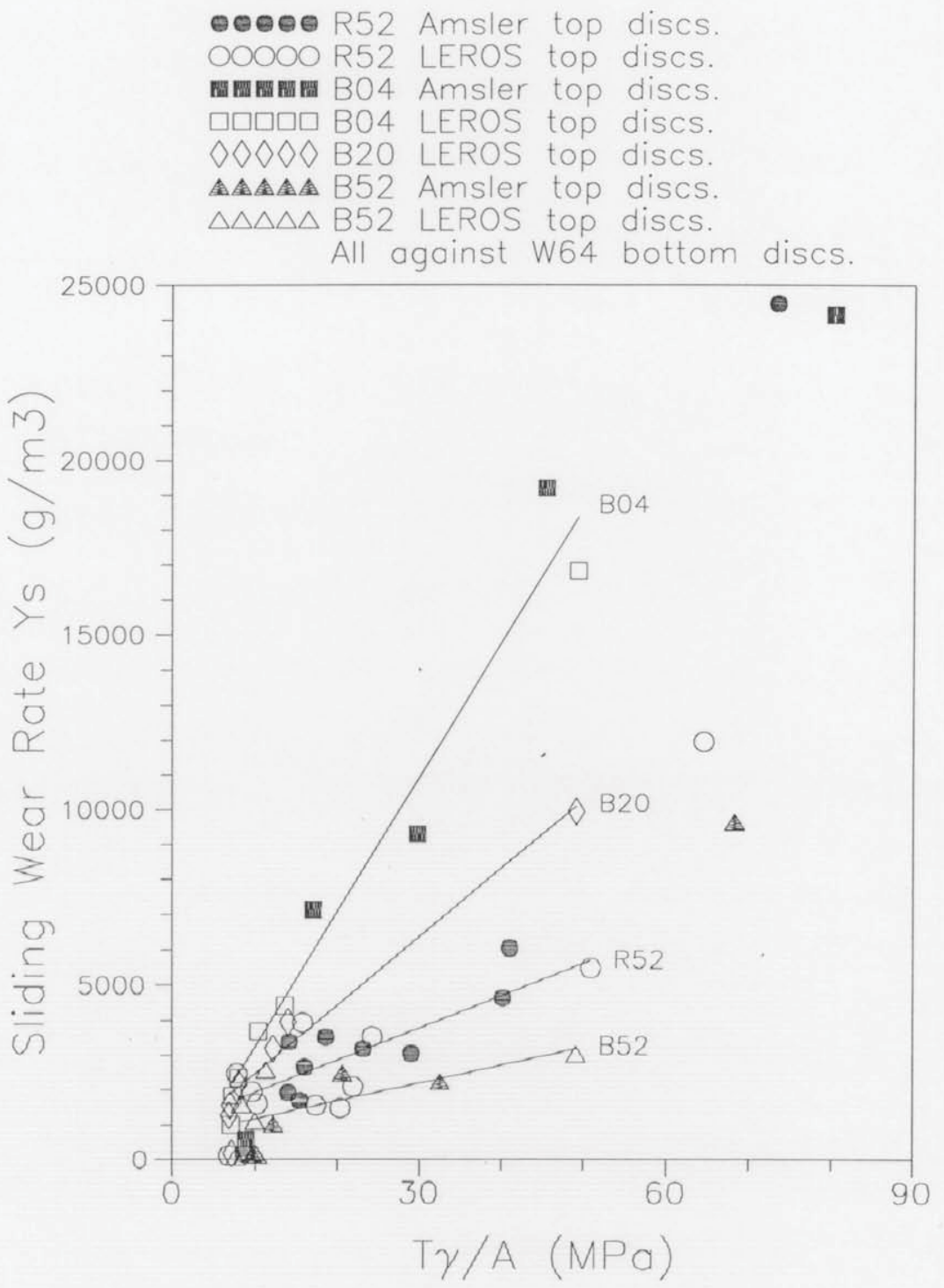


**Figure 10.6** Sliding wear rate $Y_s$ plotted linearly against $T\gamma/A$ for top (driven, "braking") discs except those with mild wear rates (less than 200 g/m$^3$).

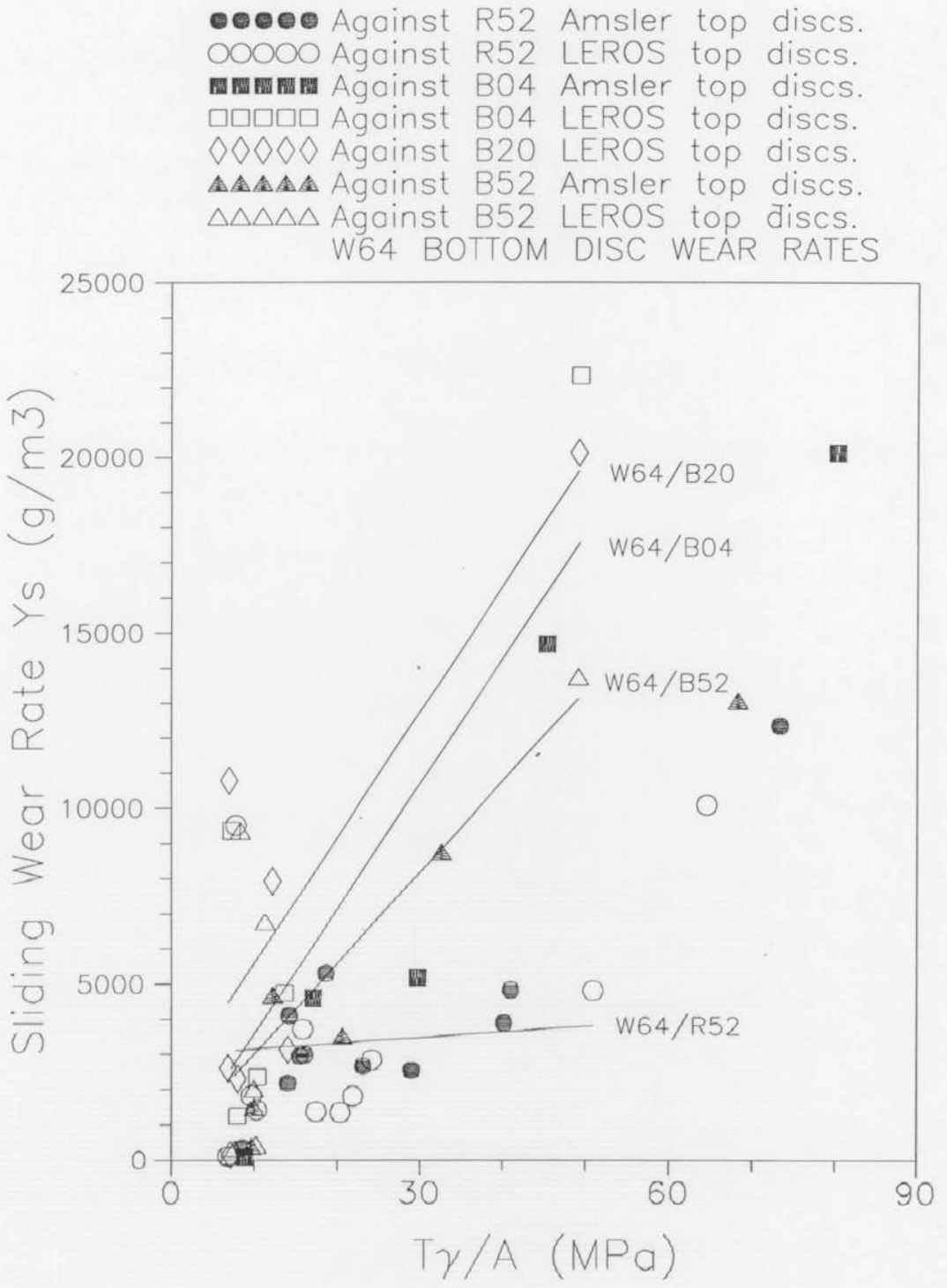


**Figure 10.7** Sliding wear rate $Y_s$ plotted linearly against Tγ/A for bottom (driving) W64 discs except those run against top discs with mild wear rates (less than 200 g/m$^3$).

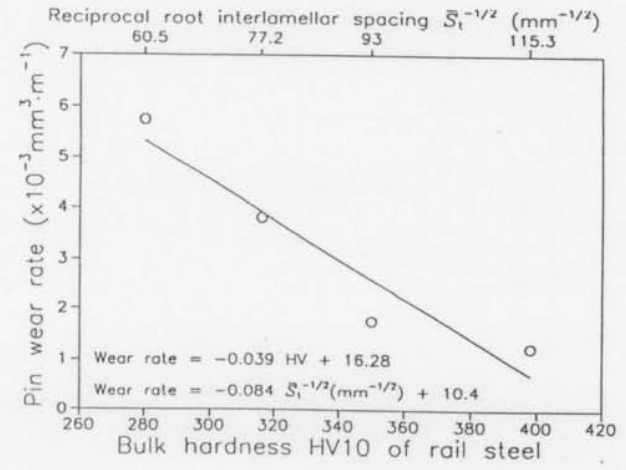


(a)

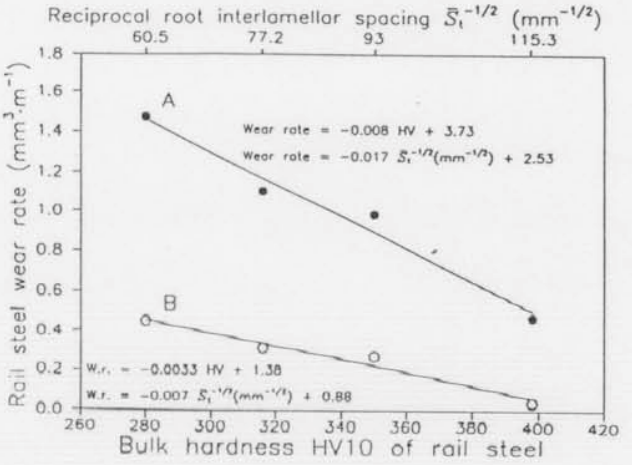


(b)

**Figure 10.8** The relationship between pearlitic rail steel wear and interlamellar spacing for different types of wear test[from Perez & Beynon, 1993].

(a) Pure sliding (rail steel pin on wheel steel disc test) wear rate of pearlitic rail steels, as volume lost per distance slid, against bulk hardness and interlamellar spacing. (Tests at 20 MPa $p_o$, 0.1 m/s speed.)

(b) Rolling-sliding wear rate (on LEROS) of pearlitic rail driven steel discs, as volume lost per distance slid, against bulk hardness and interlamellar spacing. (All tests against pearlitic wheel driving discs; "A" at 1300 MPa $p_o$, 3% $\gamma$; "B" at 500 MPa $p_o$, 10% $\gamma$.)

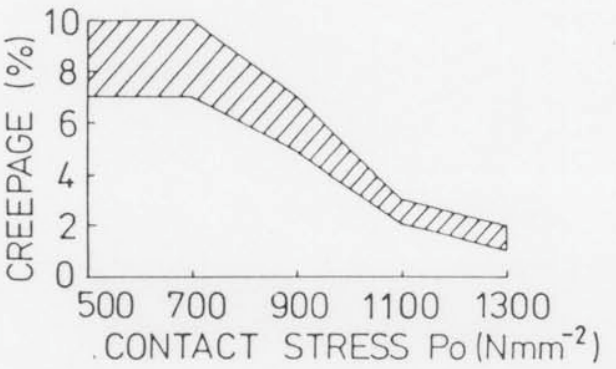


**Figure 10.9** Transition zone, with respect to test conditions, from type I, "mild" wear to type II "severe" wear for standard BS11(0.53wt.%C) rail steel. From Bolton and Clayton's Amsler test results[Bolton & Clayton, 1984].

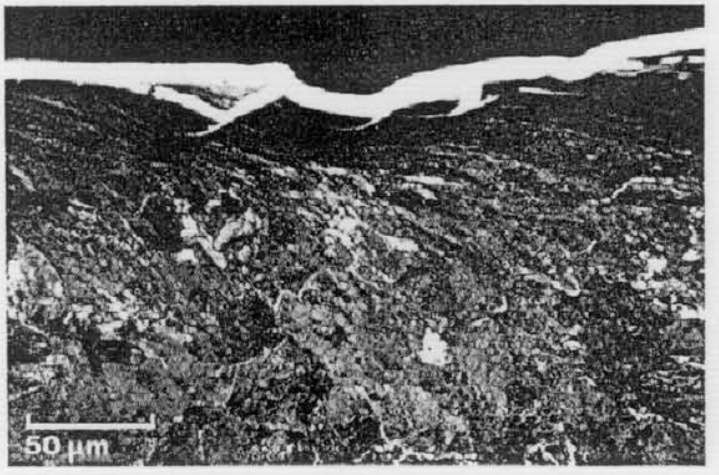


**Figure 10.10** Optical micrograph of circumferential section through a type III, "catastrophic" wear, Amsler disc (0.62wt.%C UICB rail steel). From Bolton and Clayton's Amsler test results[Bolton & Clayton, 1984].